Quantum Drude Oscillator Model for Describing the Interaction of Excess Electrons with Water Clusters: An Application to $(H_2O)_{13}^-$ †

Thomas Sommerfeld* and Kenneth D. Jordan

University of Pittsburgh, Department of Chemistry, and Center for Molecular and Materials Simulation, Chevron Science Center, 219 Parkman Avenue, Pittsburgh, Pennsylvania 15260

Received: July 8, 2005; In Final Form: September 15, 2005

Cluster anions for which the excess electron occupies an extended nonvalence orbital can be described by use of a model Hamiltonian employing quantum Drude oscillators to represent the polarizable charge distributions of the monomers. In this work, a Drude model for water cluster anions is described and used to investigate the $(H_2O)_{13}^-$ cluster. Several low-energy isomers are characterized, and the finite-temperature properties of the cluster are investigated by means of parallel tempering Monte Carlo simulations. Two structural motifs, one with double-acceptor water monomers and the other with four-membered rings of double-acceptor single-donor monomers with four free OH groups pointed in the same direction, are found to lead to large ($\gtrsim$1 eV) electron binding energies. The distributions of the computed vertical detachment energies qualitatively reproduce the experimentally measured photoelectron spectrum, and our simulations indicate that both of the main peaks in the measured spectrum derive from several isomers.

Introduction

Despite the long standing interest in water cluster anions, their geometrical structures and electron binding motifs are still poorly understood for any but the smallest clusters (for recent work see refs 1−5). Experimentally, these species are especially challenging due to complications presented by the existence of multiple isomers with similar electron binding energies and by the ill-defined cluster temperature. On the theoretical side, a major obstacle is the large contribution of dispersion and higher-order electron correlation effects to the electron binding energies.[6]

The binding energy of an excess electron to a water cluster can be partitioned into electrostatic, polarization, and electron correlation contributions, with the correlation contribution being further partitioned into second-order dispersion, second-order nondispersion, and higher-order contributions.[7,8] The smaller $(H_2O)_n^-$ clusters have been investigated using high level ab initio methods, and substantial electron correlation contributions to the binding energies of the excess electron have been found.[6,9−11] For example, for various dipole-bound isomers of $(H_2O)_6^-$, electron correlation effects have been found to account for between 40 and 65% of the net electron binding energy.[9] In clusters with small net dipole moments, the electron correlation contribution to the electron binding is even more important. Moreover, high-order correlation effects not recovered at the second-order Møller−Plesset perturbation theory[12] (MP2) level are generally substantial, necessitating the use of methods such as coupled cluster theory with single, double, and noniterative triple substitutions (CCSD(T)).[12] This effectively limits the size of the $(H_2O)_n^-$ clusters that can be accurately characterized using ab initio methods to those with seven or fewer water monomers.

To characterize larger $(H_2O)_n^-$ clusters with all-electron approaches, one is forced to use less computationally demanding methods, in particular, MP2 or density functional theory (DFT). While the MP2 method does include dispersion interactions between the excess electron and the water molecules, it ignores the high-order correlation corrections that have been found to be important in many excess electron systems[7,13] and it can fail to describe those anions for which the zeroth-order (Hartree−Fock) wave function does not bind the electron. DFT methods, on the other hand, fail to treat long-range dispersion interactions and exhibit an unphysical asymptotic interaction between the neutral molecule and an excess electron (see, e.g., ref 14). DFT methods can nevertheless give electron affinities in respectable agreement with experiment for certain species, in particular, for neutral radicals, provided small basis sets are used.[15,16] However, DFT electron binding energies have been shown to be unreliable for weakly bound anions[16,17] as well as for systems where an excess electron is attached to a closed-shell neutral species.[18] For excess electrons interacting with polar molecules and their clusters, DFT methods such as Becke3LYP[19] tend to considerably overestimate the electron binding energies, even though dispersion interactions are neglected.

Given the extended nature of the excess electron bound to water clusters, water films, and bulk water, several researchers have been motivated to develop one-electron model potentials for describing these systems. With the exceptions of the Drude model introduced by our group[6,9,20−22] and a closely related approach of Sindelka and Jungwirth,[23] none of these models include explicitly dispersion-like correlation contributions to the electron binding.

The theory behind the Drude model for excess electron systems is described in section 2 of this paper, with the specific Drude model for water cluster anions being described in section 3. This model is then applied to characterize several low-lying isomers and to calculate the finite temperature properties of the $(H_2O)_{13}^-$ cluster, with the results being described in section 4.

Drude Model

Molecular and cluster anions can be divided into two classes: those in which the excess electron attaches in a valence-

† Part of the special issue "Jack Simons Festschrift".

* To whom correspondence should be addressed. E-mail: thomas@theory.chem.pitt.edu.

10.1021/jp053768k CCC: $30.25
Published on Web 10/20/2005

type orbital and those in which it attaches in an extended nonvalence orbital and where the electron binding is dominated by a combination of long-range electrostatic, polarization, and dispersion interactions. Examples of the latter class of anions include dipole-bound and polarization-bound negative ions.[6,24−26] As discussed in the Introduction, dispersion-type interactions between the excess electron and the valence electrons of the monomers make a large contribution to the electron binding energy in such systems, and their inclusion is therefore crucial for any successful description—ab initio or model potential—of these species. As shown by Wang and Jordan, these interactions can be recovered by a model potential employing quantum Drude oscillators.[6,20] A Drude oscillator consists of two point particles with equal mass and opposite charges $+q_D$ and $-q_D$ that interact with each other through a harmonic potential with force constant k_D. The oscillator can polarize in an external field creating a dipole, and the associated polarizability is $\alpha_D = q_D^2/k_D$.

The model Hamiltonian for an electron interacting with one or more Drude oscillators is

$$H_D = H_e + H_{osc} + V_{e,osc} \tag{1}$$

where H_e and H_{osc} are the Hamiltonians of the electron and of the collection of Drude oscillators, respectively, and $V_{e,osc}$ describes the interaction between the electron and the Drude oscillators. The electronic Hamiltonian

$$H_e = -\frac{\hbar^2}{2m_e}\nabla_e^2 + V_{es} + V_{rep} \tag{2}$$

includes the kinetic energy operator and a pseudopotential that consists of an electrostatic part, V_{es}, and a short-range repulsion, V_{rep}. The Hamiltonian for the collection of Drude oscillators is

$$H_{osc} = \sum_k \left[-\frac{\hbar^2}{2m_D}\nabla_k^2 + \frac{1}{2}k_D\,(X_k^2 + Y_k^2 + Z_k^2) + V_{es,osc} + V_{osc,osc} \right] \tag{3}$$

where $\mathbf{R}_k = (X_k, Y_k, Z_k)$ is the vector from the positive to the negative charge of Drude oscillator k, $V_{es,osc}$ represents the interaction between the charge distribution of the monomers and the Drude oscillators, and $V_{osc,osc}$ describes the interactions between the Drude oscillators. The latter two terms account for intermolecular induction and dispersion as well as for many-body polarization and dispersion interactions involving two or more Drude oscillators. Since these terms are as a rule already included in the molecular force field employed to compute the monomer−monomer interactions, it is vital to carefully avoid double counting. Intermolecular induction and dispersion can be removed from the employed force field and treated through the quantum Drude oscillators. Alternatively, induction can be treated classically and dispersion can be modeled, for example, by a Lennard-Jones potential. In this case, $V_{es,osc}$ and $V_{osc,osc}$ should be removed from H_{osc} and V_{es} should be modified to include the interaction of the excess electron with the charge distribution of the *interacting* monomers. As will be discussed below, we adopt the latter strategy for studying $(H_2O)_{13}^-$.

In the following, we assume that the cluster is comprised of one type of molecule, for example, water, in which case, the same force constant k_D and the same reduced mass m_D is employed for each oscillator. In the case of mixed clusters, different values of k_D and m_D can be associated with the different species. In addition, separate force constants can be introduced for different directions to allow for the anisotropy of the molecular polarizability. The electron−oscillator coupling is given by

$$V_{e,osc} = \sum_k q_D \frac{\mathbf{r}_k\cdot\mathbf{R}_k}{r_k^3} f(r_k) \tag{4}$$

where $\mathbf{r}_k$ is the vector from the electron to Drude oscillator k, and $f(r)$ is a damping function introduced to cut off the unphysical short-range behavior. To facilitate integral evaluation when using Gaussian-type basis sets, we use $f(r) = 1 - \exp(-br^2)$, where b is a parameter, chosen as described below.

To set up a Drude model for a particular excess electron system, one needs to specify the various terms in H_D as well as the potential energy function for the underlying neutral system. For example, for water cluster anions, one first chooses a suitable model potential for describing the water−water interactions. Typical force fields employ a set of point charges and, sometimes also, distributed higher multipoles, to represent the electrostatics, as well as Lennard-Jones or similar terms to account for the intermolecular dispersion and short-range repulsion. It is important that the molecular model for the neutral system also explicitly includes polarizability, since one can then simply replace the polarizable sites with Drude oscillators.

We emphasize that, although the Drude model treats only the excess electron explicitly, it is still many body in nature since the Drude oscillators are also treated quantum mechanically. In essence, each water monomer is modeled by a pseudopotential together with a three-dimensional (3D) Drude oscillator. One-particle basis sets are introduced for the excess electron and for each Drude oscillator, and the many-body wave function is represented in terms of the products of the electron and oscillator one-particle functions. The basis sets used in the $(H_2O)_{13}^-$ study as well as several technical aspects associated with computing the many-body wave function will be discussed in the next section.

Methodological Aspects

In this section, we describe the Drude model that was introduced by Wang and Jordan for modeling water cluster anions.[9,21] We start with a summary of the water model and pseudopotential used for describing the electron−water interactions. Then the choice of one- and many-particle basis sets and other technical aspects relevant to efficient computation of the lowest eigenvalues of H_D are discussed.

The water−water interactions were modeled using the rigid-monomer Dang−Chang potential.[27] This model employs three point charges: +0.519 on each H atom and −1.038 on the so-called M site, located on the rotational axis, 0.215 Å from the O atom in the direction of the H atoms. A 6-12 Lennard-Jones interaction is included between the O atoms of different monomers, and an isotropic polarizable site with a polarizability equal to the experimental value of 1.444 Å^3 is also located at the M site.

In the present work, we adopt the strategy of Wang and Jordan[9] and describe the intermolecular induction due to the interactions of the polarizable sites with the charges on other water monomers and with each other by solving the classical polarization equations. The electronic Hamiltonian H_e (eq 2) then includes in V_{es} both the Dang−Chang charges and the induced dipoles from intermolecular induction. The repulsive potential V_{rep} is constructed using the procedure of ref 28. The

resulting $V_{es} + V_{rep}$ potential is too attractive, and following ref 21, V_{rep} is scaled by a factor of 6.8 so as to reproduce the electrostatic binding energy of an excess electron to the water dimer. Finally, a Drude oscillator is placed at the M site of each water monomer. A perturbation theory analysis[6] shows that the electron−Drude oscillator interaction energy is relatively insensitive to the choice of the force constant, k_D, or reduced mass, m_D, of the Drude oscillators. Therefore m_D and q_D are arbitrarily chosen to be the mass and charge of an electron, respectively, and k_D is chosen such that the resulting polarizability α_D is identical to the experimental value of an isolated water molecule, that is, $k_D = 0.103$ au. The parameter b in the damping function is adjusted so that the Drude model reproduces the electron binding energy of the water dimer obtained from a large basis set CCSD(T) calculation, giving $b = 0.43$.[21] Thus, the Drude model for water cluster anions has only two free parameters which are fixed using ab initio electrostatic (Koopmans' theorem)[29] and CCSD(T) electron binding energies of the water dimer.

We now turn to the choice of the one-particle basis sets for the electron and the Drude oscillators. The sizes of the basis sets for the electron, N_e, and for each oscillator, N_{osc}, obviously determine the size of the many-body expansion and therefore the computational cost of the Drude model calculations. Minimizing the computational cost is an important consideration due to the intended use of the Drude model in carrying out finite-temperature Monte Carlo simulations of water cluster anions, where millions of configurations need to be generated. In the present study of $(H_2O)_{13}^-$, the "minimal" oscillator basis set from ref 9, which consists of the ground state and the triply degenerate lowest excited state of the harmonic oscillator ($N_{osc} = 4$), is employed for each Drude oscillator. We note that this "minimal" set gives satisfactory results provided water−water induction is treated classically.[9] A larger oscillator basis set would be required if the quantum Drude oscillators were also employed to describe the water−water interaction.[9,21]

The electronic basis set is taken to consist of Gaussian-type functions. Wang and Jordan have shown that a basis set, comprised of a floating 5s4p set of diffuse Gaussians together with 2s1p sets of Gaussians on each H atom, is suitable for describing the binding of the excess electron to a wide range of geometrical structures for small water clusters.[9] This basis set, here denoted as basis I, employs 10 functions per water monomer in addition to those associated with the floating set. Test calculations on clusters containing 10−30 monomers show that it suffices to place the floating basis functions at the center of mass of the cluster, although it may be necessary to employ additional floating functions when treating still larger clusters.

The computational effort for clusters containing 10 or more monomers is determined primarily by the size of the monomer-centered basis set. This led us to explore the possibility of designing a smaller monomer-centered basis set. After considerable experimentation, we derived basis set II consisting of only six Gaussian functions per water monomer. Basis II is comprised of one s function on each H atom and one sp set centered at the midpoint between the H atoms. When combined with the 5s4p set of diffuse Gaussians located at the center of mass, basis II gave electron binding energies in close agreement with those obtained with the larger basis I. Our test calculations led to the following exponents for the molecule-centered basis functions: 0.015 for the s functions on the H atoms and 0.26 and 0.09, respectively, for the s and p functions located at the midpoint between the H atoms. The adoption of basis set II in place of basis set I for the excess electron results in about a factor of 3 reduction in the computational time required for Drude model calculations on water clusters containing over 10 monomers.

Having established one-particle basis sets for the Drude oscillators and for the excess electron, we now consider the many-particle basis set. A configuration interaction (CI) approach is used to expand the wave function of the electron and the Drude oscillators in a direct product basis

$$\Psi(\mathbf{r},\mathbf{R}^{(1)},\mathbf{R}^{(2)},\cdots) = \sum_{\alpha,n,m,\cdots} c_{\alpha,n,m\cdots}\phi_\alpha(\mathbf{r})\chi_n^{(1)}(\mathbf{R}^{(1)})\chi_m^{(2)}(\mathbf{R}^{(2)})\cdots \tag{5}$$

where ϕ_α is an electron orbital, $\chi_n^{(k)}$ is the nth harmonic oscillator state of the kth Drude oscillator, and $c_{\alpha nm\cdots}$ is the associated CI coefficient. The CI expansion is restricted so that at most one oscillator is excited, that is, only the $|\alpha 0\rangle$ and $|\alpha n^{(k)}\rangle$ configurations, where the electron occupies an arbitrary orbital ϕ_α and all oscillators are in their respective ground states $\chi_0^{(k)}$ or the kth oscillator is excited to its nth state, are included. A consequence of this restriction is that the calculations retain only two-body polarization and dispersion interactions between the excess electron and the water monomers.

Note that the CI wave function is independent of the particular choice of electronic orbitals ϕ_α (provided the same basis set is used to expand the orbitals). We normally use the canonical orbitals that diagonalize the electronic Hamiltonian H_e, since this choice leads to a particularly sparse matrix representation of H_D, as discussed below. We could, however, equally well use directly the (orthogonalized) Gaussian basis functions with all the advantages localized basis sets offer for extended systems.

An important consequence of the adoption of the CI approach for calculating the electronic energy is that it is also applicable to anions for which the cluster's electrostatic potential alone is unable to bind an excess electron. If a molecule or cluster can bind an excess electron, but the corresponding electrostatic potential including intermolecular induction does not, even correlated ab initio methods such as MP2 or CCSD(T) can fail to predict electron binding owing to the inadequacy of the Hartree−Fock wave function (see ref 30 for an example).

With the choice of the canonical orbitals of H_e as the electronic basis set, that is

$$H_e\phi_\alpha = \epsilon_\alpha\phi_\alpha \tag{6}$$

the CI representation of H_D has an especially simple structure, with H_e and H_{osc} contributing only to the diagonal elements and all off-diagonal elements being due to $V_{e,osc}$. The sparseness of the CI matrix is most clearly seen when its coarse "block" structure is considered, where the $|\alpha 0\rangle$ configurations (all oscillators in their ground states) form block 0 and configurations where the kth oscillator is excited, $|\alpha m^{(k)}\rangle$, form block n (Figure 1). At the block level, $V_{e,osc}$ couples only block 0 to all other blocks, while the coupling matrix elements within the diagonal blocks and between two different "oscillator-excited" blocks vanish, that is

$$\langle\alpha 0|V_{e,osc}|\beta 0\rangle = 0$$

$$\langle\alpha 0|V_{e,osc}|\beta n^{(k)}\rangle \neq 0$$

$$\langle\alpha m^{(l)}|V_{e,osc}|\beta n^{(k)}\rangle = 0 \tag{7}$$

The resulting CI matrix is shown schematically in Figure 1. The sparse structure of the matrix derives from the factorization of the 6D coupling integrals into 3D integrals over either the electronic coordinates or oscillator displacement coordinates.

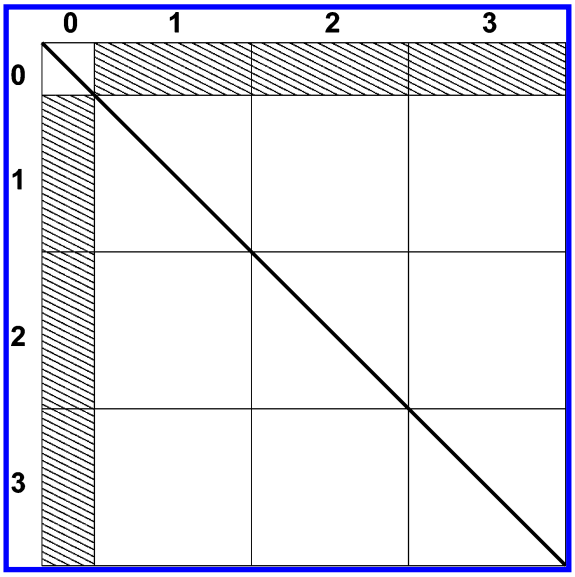

Figure 1. Schematic representation of the Drude model CI matrix for the water trimer. The configurations are classified according to which Drude oscillator is excited, where **0** refers to configurations $|\alpha 0\rangle$ with all oscillators in their respective ground states, **1** refers to configurations $|\alpha n^{(1)}\rangle$, where oscillator 1 is excited, etc. With the use of the basis sets described in the text, the CI matrix is very sparse. Apart from the diagonal, only the **0**−**k** coupling blocks are occupied.

If larger basis sets were used for the Drude oscillators, some nonzero matrix elements would appear in the diagonal blocks, however, the character of the off-diagonal blocks would be unchanged. In contrast, the electronic basis functions influence the matrix structure only at a sub-block level but have no influence on the coarse structure. Thus, the Drude model CI matrix has, in general, a "super-arrow" structure similar to Figure 1, and it is this structure that can be used with great advantage in the iterative diagonalization methods (Lanczos-Arnoldi and Davidson[31]) that we use to compute the lowest few eigenvalues of H_D. If canonical electronic orbitals and the minimal oscillator basis set are used, it is straightforward to compute the number of nonzero matrix elements. For $N_W \gg 1$, where N_W is the number of water monomers, the number of nonzero elements is proportional to $N_W N_e^2$ and the fraction of nonzero elements is $2/3N_W$. For clusters containing more than 10 monomers, N_e itself is essentially proportional to N_W owing to the monomer-centered basis functions. Thus, although the matrix dimension is growing as N_W^2, the number of nonzero elements and the overall computational effort are only cubic functions of cluster size.

Before we turn to the application to $(H_2O)_{13}^-$, it is useful to briefly discuss the timings and bottlenecks in a typical calculation. As an example, consider a calculation for a $(H_2O)_{24}^-$ cluster on a 1.5 GHz Athlon processor. The electronic basis set consists of 161 Gaussian functions, and the dimension of the CI matrix is 11 753. In the one-particle part of the problem, the most time-consuming step is the evaluation of the integrals associated with the potentials in H_e, requiring roughly 4 s. Diagonalization of H_e in the Gaussian basis set takes only 0.15 s, and the time spent to evaluate the water−water interactions and to set up the Hamiltonian for the Drude oscillators is negligible. In the many-particle part of the problem, it takes about 0.5 s to compute the coupling matrix elements and to transform them into the ϕ_α basis; building the CI matrix and computing its lowest eigenvalue takes about 0.9 s. In Monte Carlo simulations involving only moves of single water molecules, only a subset of the integrals needs to be evaluated further speeding up the calculations. The total CPU time is on the order of 6 s per structure, and thus, Drude model calculations for $(H_2O)_{24}^-$ are several orders of magnitude faster than ab initio or density functional calculations on a cluster of this size.

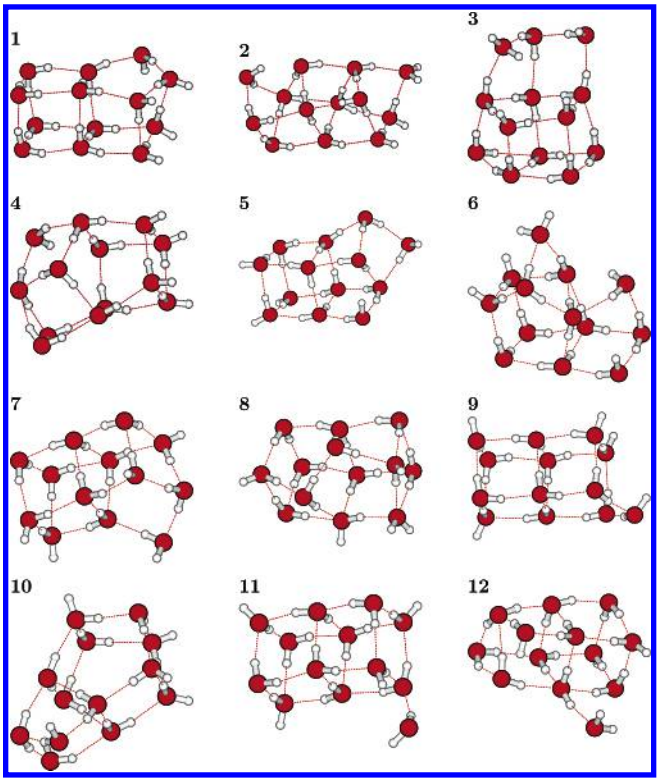

Figure 2. Structures of selected low-energy isomers of $(H_2O)_{13}^-$.

$(H_2O)_{13}^-$ Cluster

$(H_2O)_{13}^-$ is the smallest negatively charged water cluster that displays two well separated peaks in its photoelectron spectrum,[1] indicating the presence of at least two isomers in the experiments. Using the Drude model described in the previous section, we have carried out parallel-tempering Monte Carlo (PTMC) simulations[32] on $(H_2O)_{13}^-$. In the following discussion, we highlight the main findings from these simulations. We first examine the structures and electron binding energies of several low-energy isomers identified in the simulations and then consider the electronically excited states of a prototypical isomer. Finally, we consider the temperature dependence of the electron binding energies of the clusters.

Minimum energy structures were obtained by numerical geometry optimizations of randomly selected configurations sampled at various temperatures in the PTMC simulations. Twelve low-energy isomers are displayed in Figure 2, and the relative potential energies of the anions, the associated electron binding energies, and the dipole moments of the corresponding neutral clusters are reported in Table 1. All low-energy isomers shown in Figure 2 have 21 hydrogen bonds. Isomers with fewer hydrogen bonds tend to have more open structures, and the most stable isomer having only 20 hydrogen bonds is calculated to lie energetically 235 meV above the lowest energy isomer **1** (cf. Table 1).

Apart from isomer **11**, the neutral frameworks of the low-energy anionic isomers possess substantial dipole moments, and as a result, these cluster anions can be classified as dipole-bound species.[6,24] Isomer **11** is an exception in that the electrostatic potential of its neutral framework is not sufficiently strong to bind the excess electron, although the many-particle Hamiltonian

TABLE 1: Relative Energies and Electron Binding Energies of the Isomers of $(H_2O)_{13}^-$ Displayed in Figure 2[a]

isomer	relative stability (meV)	electron binding energy (meV)[b] ES	PT2	CI	dipole moment[c] (debye)
1	0	711	1145	1340	20.6
2	18	637	1021	1170	19.2
3	46	568	1038	1246	12.8
4	52	596	982	1168	17.8
5	109	258	510	701	11.2
6	158	523	905	1107	14.2
7	183	99	255	458	7.4
8	190	610	1048	1224	14.6
9	191	95	250	450	7.3
10	208	167	368	564	10.7
11	311	~0	~0	138	2.4
12	328	135	360	633	9.1

[a] All results have been obtained using the Drude model described in section 3. [b] The electron binding energies have been computed at three levels: using the electrostatic interactions (and short-range repulsion) only (ES), through second-order perturbation theory (PT2), and including many-body effects through a CI wave function. An electron binding energy ~0 implies that the excess electron is not bound at this level of theroy (see text). [c] The dipole moments are that of the corresponding neutral clusters.

H_D (eq 1) does support a strongly bound state. (Actually, since the dipole moment of the corresponding neutral cluster is 2.4 debye, in an infinite basis set, H_e would support a bound state, albeit with an electron binding energy much less than 1 meV.) Consequently, we characterize this anion as a polarization/dispersion bound state.

With the exception of **7**, the isomers depicted in Figure 2 are the lowest energy members of families of similar structures, sharing the arrangement and connectivity of O atoms. Different isomers of a family can be generated by one or more donor−acceptor exchanges. Since the dipole moments of the monomers are arranged differently in different family members, their total dipole moments, their electron binding energies, and their total energies are in general substantially different; isomers **1** and **7** are an example.

Isomers **1**, **5**, **7**, **8**, **9**, **11**, and **12** can be viewed as being derived from the addition of a water monomer (and an electron) to a fused cubic form of $(H_2O)_{12}$,[33] and low-dipole isomers of these families form a substantial subset of the low-energy minima of neutral $(H_2O)_{13}$. In particular, **8** is a member of the family of clusters including the global minimum of neutral $(H_2O)_{13}$.[34] The differences between typical structures for neutral and anion clusters can be understood as follows. For the neutral clusters, the lowest energy isomers generally have rather small dipole moments. On the other hand, the electron binding energy generally increases with dipole moment, and in most cases, the enhanced electron binding energy more than compensates for the energetic cost of the donor−acceptor exchanges that enhances the dipole moment.

For the dipole-bound anions listed in Table 1, between 21 and 54% of the electron binding derives from the electrostatic interactions, roughly 35% is due to dispersion interactions and is recovered in second-order perturbation theory, and the remaining binding derives from higher-order correlations between the excess electron and the Drude oscillators. Figure 4 displays the electron distribution of isomer **4** calculated, on one hand, accounting for electrostatic effects only and, on the other hand, at the CI level which includes dispersion and higher-order correlation effects as well. The electron density obtained from the CI calculation is much more compact than that from calculations accounting for electrostatic interactions only.

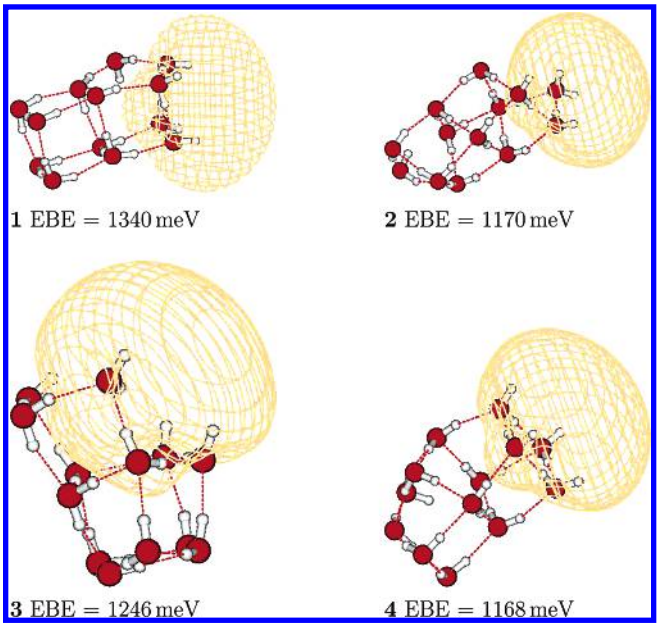

Figure 3. Distribution of the excess electron for isomers **1**, **2**, **3**, and **4** of $(H_2O)_{13}^-$. The pictures show iso-surfaces of the natural orbitals of the reduced CI density. The occupation numbers of these orbitals are between 0.96 and 0.98. The iso-surfaces have been drawn at a value of 0.0141 bohr$^{-3/2}$ and contain roughly 70% of the electron density.

Interestingly, the electron distribution from the Drude model calculations including second-order correlation corrections only (not shown) is very similar to that from the purely electrostatic calculations. Moreover, at the CI level, a significant fraction of the electron density is predicted to be localized inside the cluster. As pointed out previously by Wang and Jordan, this contraction of the electron density is due to configurations in which the electron is excited but the Drude oscillators are in their ground state. These single excitations do not contribute to the second-order energy but enter into the CI wave function by mixing with the double excitations responsible for the dispersion interactions between the excess electron and the Drude oscillators.[21]

The isomers with large (≳1 eV) electron binding energies can be grouped into two classes. Isomers of the first class possess a surface tetramer with four double-acceptor single-donor monomers with all four dangling hydrogens pointing away from the cluster that serves as the site of electron attachment. Examples include isomers **1** and **4** (Figure 3). The second class of isomers possessing high electron binding energies has a double (AA)- or triple (AAA)-acceptor water monomer with two free OH groups, with the excess electron bound in the vicinity of this monomer. Isomers **2**, **3**, and **6** have AA water monomers, and isomer **8** has a AAA monomer. Recently, the Johnson group has concluded on the basis of their vibrational spectra[3] that the dominant isomers observed for $(H_2O)_{4-6}^-$ clusters all possess a AA water monomer. In neutral water clusters, the presence of triple-acceptor water molecules is quite rare (see ref 34 for a low-energy isomer of $(H_2O)_{21}$ with a triple-acceptor double-donor water molecule). However, in the anionic water clusters, a AAA monomer can be stabilized as a consequence of an enhanced binding of the excess electron.

The triple-acceptor isomer **8** supports three electronically excited bound states with electron binding energies of 235, 75, and 45 meV, whereas, for example, the double-acceptor structure **6** supports only two bound excited states (binding energies of 165 and 55 meV). The electron distributions of the ground and three excited states of **8** are shown in Figure 5. The ground state anion has essentially s character with the triple-acceptor

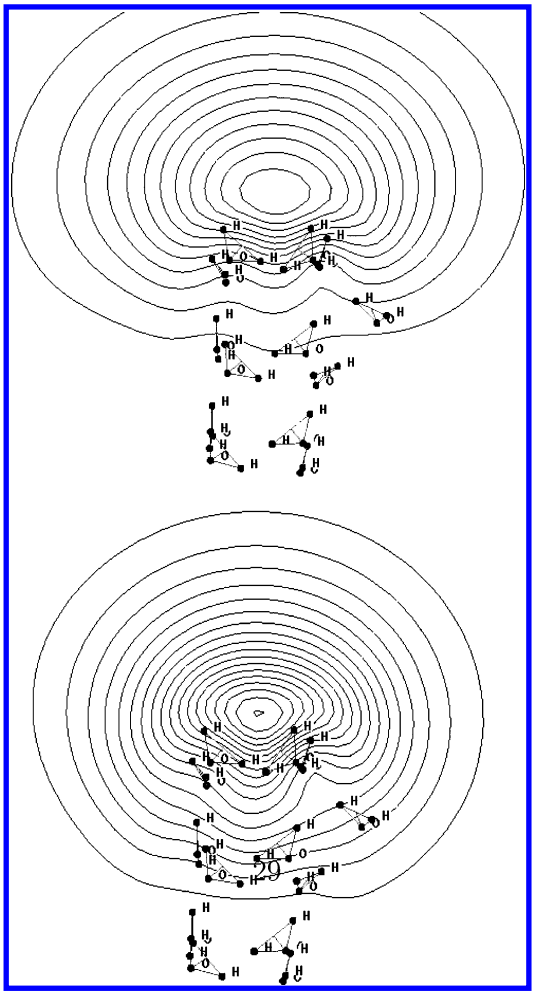

Figure 4. Cut through the electron density of isomer **4** of $(H_2O)_{13}^-$. The density plotted in the upper panel is that of the electron bound by electrostatic interactions alone (density from the ground state of H_e), and that plotted in the lower panel has been obtained at the CI level (reduced density associated with the ground state of H_D). Contours start at and increase in steps of 6.25×10^{-6}. In the upper panel, the innermost contour is 9×10^{-4}; in the lower panel, it is 2.025×10^{-3}.

water monomer being located close to the center of the charge distribution, whereas the three excited states are p-like in character with the energy splitting being due to the nonsymmetrical environment of the cluster.

The measured photoelectron spectrum of $(H_2O)_{13}^-$ displays a broad double peak structure with maxima at 0.5 and 0.85 eV, a shoulder at 0.2 eV, and a total width of about 1 eV.[1] This structure has been interpreted in terms of surface-bound and interior-bound species causing the low- and high-binding energy peaks, respectively.[1] The Drude model calculations suggest an alternative interpretation: namely, that both peaks in the photoelectron spectrum are due to surface-bound states. The high-binding energy peak, which is centered at 0.85 eV and extends to 1.3 eV, is likely due to a large number of different isomers some with double- or triple-acceptor monomers and others with four-membered rings with all four monomers having dangling H atoms pointed in the same direction as **1** and **4**. We have also found many isomers of $(H_2O)_{13}^-$ with electron binding energies between 0.45 and 0.8 eV. Most of these have three adjacent surface waters with dangling H atoms; examples are **9** and **10**. Thus, it is likely that the peak centered near 0.5 eV in the photoelectron spectrum is due to this class of isomers.

We now turn to the results of the Monte Carlo simulations of the finite temperature behavior of $(H_2O)_{13}^-$. These simulations

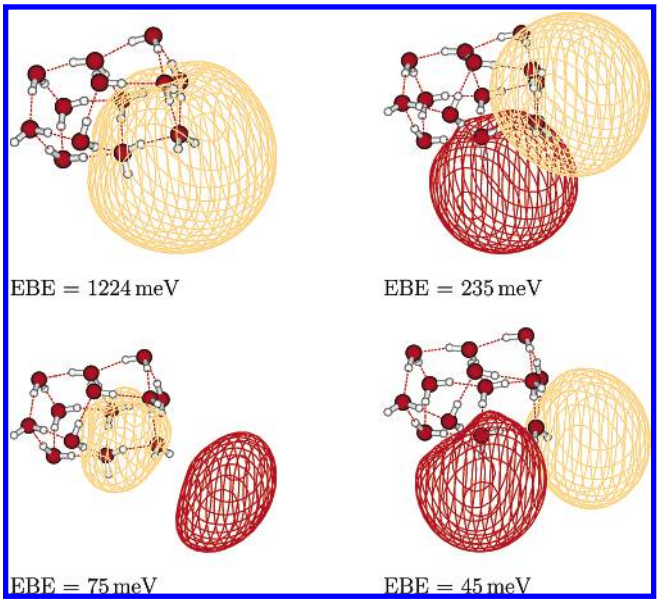

Figure 5. Natural orbitals of the ground and three excited states of the $(H_2O)_{13}^-$ isomer **8**. The figure plots iso-surfaces of the natural orbitals of the reduced CI density. The occupation numbers of these orbitals are between 0.95 and 0.98. The iso-surfaces have been drawn at a value of 0.01 bohr$^{-3/2}$.

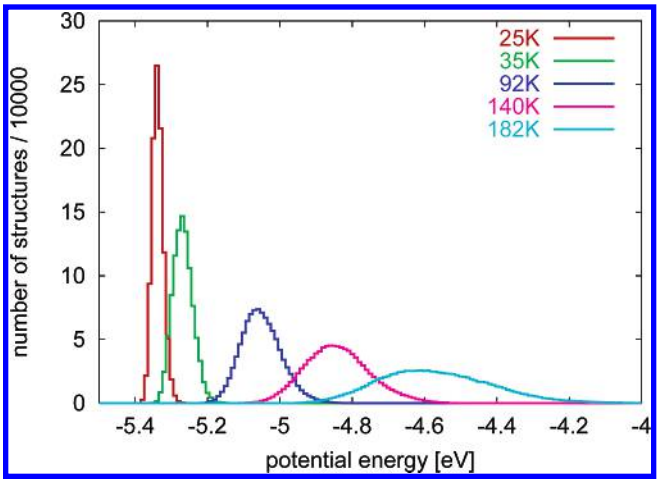

Figure 6. Potential energy distributions of $(H_2O)_{13}^-$ at selected temperatures. The results have been obtained using the Drude model for water cluster anions in conjunction with the PTMC method employing 20 temperatures between 25 and 260 K. Two million production moves were made at each temperature. The resulting potential energies were sorted into bins of 10 meV width.

were carried out using the Drude model to calculate the energies and the parallel-tempering Monte Carlo procedure[32] to avoid quasi-ergodic behavior. After the replicas were alllowed to equilibrate for one million moves, two million production moves were carried out for each of 20 replicas at temperatures ranging from 25 to 260 K.[35] Most moves in each replica involve single monomers with the probability of acceptance being established by the Metropolis criterion.[36] Every 250 moves an attempt was made to exchange configurations between adjacent temperature replicas. With the chosen temperatures,[35] the success rates of the exchange moves were about 40%. The potential energy distributions of the structures sampled at selected temperatures are shown in Figure 6.

All 60 million structures encountered during the simulation have positive electron binding energies; in other words, there were no autodetachment events at any of the temperatures employed. In contrast, dissociation of water molecules is found

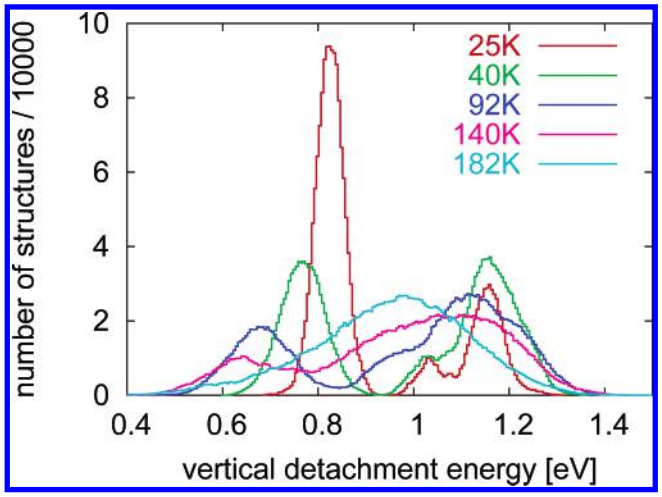

Figure 7. Electron binding energy of distributions $(H_2O)_{13}^-$ at selected temperatures. The results have been obtained using the Drude model in conjunction with the PTMC method employing 20 temperatures between 25 and 260 K. Two million production moves were made at each temperature. The resulting electron binding energies were sorted into bins of 5 meV width.

to occur in the replicas with temperatures above 200 K. These evaporative events were suppressed by use of a constraining potential. The experimentally observed $(H_2O)_{13}^-$ clusters are expected to have temperatures less than 150 K in the absence of attached Ar atoms and to be much colder than this ($T \approx 50$ K) in the presence of attached Ar atoms. The purpose of the replicas with $T > 150$ K in the PTMC simulations is to avoid trapping in configurational space in the low-temperature replicas.

The distributions of electron binding energies calculated at five selected temperatures are shown in Figure 7. At $T = 25$ K, the population shows three discernible peaks at 0.8, 1.05, and 1.15 eV. At higher temperatures, the two high-binding energy peaks merge into a single feature, and all replicas between 40 and 150 K display two prominent peaks, the upper of which is predicted to fall near 1.1 eV and the other of which drops from 0.85 to 0.65 eV and drops in intensity as the temperature increases. For the 182 K replica, there is a single broad peak, with its maximum near 0.95 eV. Qualitatively, the change in the electron binding energy distributions with temperature is similar to that in the measured photoelectron spectra. Our simulations indicate that both of the main peaks derive from several different isomers, with the assignments as discussed above.

Conclusions

In summary, a quantum Drude model has been used to investigate geometrical structures and electron binding energies of selected isomers of $(H_2O)_{13}^-$ as well as to examine how the distribution of electron binding energies depends on the cluster temperature. Dispersion and higher-order correlation effects are found to make large contributions to the electron binding energies of the clusters. Correlation effects lead up to increases in the electron binding energies ranging from a factor of 1.8 to over 5-fold depending on the isomer. As a consequence, explicit inclusion of correlation effects is essential for obtaining the correct energy ordering of different isomers. We identified 60 isomers of $(H_2O)_{13}^-$ that lie energetically within 600 meV above the global minimum and have electron binding energies ranging from 100 meV to 1.3 eV. The isomers with the highest electron binding energies show two different binding motifs: one group has a double- or triple-acceptor water monomer with two free OH bonds and the other group has a four-membered ring of double-acceptor single-donor monomers with all four free OH bonds pointing in the same direction. Electron attachment at double-acceptor sites has been established previously in water clusters with four to six monomers.[3] Several different arrangements of water monomers give binding energies in the 0.45 to 0.8 eV range, that is, in the vicinity of the lower peak centered near 0.5 eV in the measured photoelectron spectrum. These include isomers with three adjacent water molecules with free OH groups pointed in the same direction as well as isomers with a four-membered ring of AAD monomers with all free OH groups pointed in the same direction but with some of the H-bonded OH groups pointed in the opposite direction, so as to reduce the net dipole field.

The results of the present study demonstrate that it is not necessary to invoke an interior electron binding motif to account for the $(H_2O)_{13}^-$ cluster anions with high vertical attachment energies observed experimentally.[1] Turi et al. carried out simulations of $(H_2O)_n^-$, $n = 20-200$ and concluded that these species also have surface states with high electron binding energies.[37]

Acknowledgment. We dedicate this work to Professor Jack Simons in honor of his 60th birthday. The authors acknowledge several helpful discussions with Dr. Feng Wang about his implementation of the Drude code. We also acknowledge stimulating discussions with Kadir Diri and Albert DeFusco. Financial support came from the National Science Foundation.

References and Notes

(1) Verlet, J. R. R.; Bragg, A. E.; Kammrath, A.; Cheshnovsky, O.; Neumark, D. M. *Science* **2005**, *307*, 93.
(2) Jordan, K. D. *Science* **2004**, *306*, 618.
(3) Hammer, N. I.; Shin, J.-W.; Headrick, J. M.; Diken, E. G.; Roscioli, J. R.; Weddle, G. H.; Johnson, M. A. *Science* **2004**, *306*, 675.
(4) Paik, D. H.; Lee, I.-R.; Yang, D.-S.; Baskin, J. S.; Zewail, A. H. *Science* **2004**, *306*, 672.
(5) Bragg, A. E.; Verlet, J. R. R.; Kammrath, A.; Cheshnovsky, O.; Neumark, D. M. *Science* **2004**, *306*, 669.
(6) Jordan, K. D.; Wang, F. *Annu. Rev. Phys. Chem.* **2003**, *54*, 367.
(7) Gutowski, M.; Skurski, P.; Boldyrev, A. I.; Simons, J.; Jordan, K. D. *Phys. Rev. A* **1996**, *54*, 1906.
(8) Gutowski, M.; Skurski, P.; Jordan, K. D.; Simons, J. *Int. J. Quantum Chem.* **1997**, *64*, 183.
(9) Wang, F.; Jordan, K. D. *J. Chem. Phys.* **2003**, *119*, 11645.
(10) Lee, H. M.; Suh, S. B.; Tarakeshwar, P.; Kim, K. S. *J. Chem. Phys.* **2005**, *122*, 044309.
(11) Herbert, J. M.; Head-Gordon, M. *J. Phys. Chem. A* **2005**, *109*, 5217.
(12) Levine, I. R. *Quantum Chemistry*; Prentice Hall: New Jersey, 1991.
(13) Skurski, P.; Gutowski, M.; Simons, J. *Int. J. Quantum Chem.* **2000**, *80*, 1024.
(14) Weimer, M.; Sala, F. D.; Görling, A. *Chem. Phys. Lett.* **2003**, *372*, 538.
(15) Rienstra-Kiracofe, J. C.; Tschumper, G. S.; Schaefer H. F., III; Nandi, S.; Ellison, G. B. *Chem. Rev.* **2002**, *102*, 231.
(16) Jensen, F. *J. Chem. Phys.* **2002**, *117*, 9234.
(17) Jarzecki, A. A.; Davidson, E. R. *Chem. Phys. Lett.* **1999**, *300*, 44.
(18) See ref 15, sections IV.A and IV.C.
(19) Becke, A. D. *J. Chem. Phys.* **1993**, *98*, 5648.
(20) Wang, F.; Jordan, K. D. *J. Chem. Phys.* **2001**, *114*, 10717.
(21) Wang, F.; Jordan, K. D. *J. Chem. Phys.* **2002**, *116*, 6973.
(22) Šindelka, M.; Špirko, V.; Jungwirth, P.; Wang, F.; Mahalakshmi, S.; Jordan, K. D. *J. Chem. Phys.* **2004**, *121*, 1824.
(23) Šindelka, M.; Špirko, V.; Jungwirth, P. *J. Chem. Phys.* **2002**, *117*, 5113.
(24) Compton, R. N.; Hammer, N. I. In *Advances in Gas-Phase Ion Chemistry*; Adams, N. G.; Babcock, L. M., Eds.; JAI Press: Stamford, CT, 2001; Vol. 4, pp 257−305, pp 257−305.
(25) Abdoul-Carime, H.; Desfrançois, C. *Eur. Phys. J. D* **1998**, *2*, 149.
(26) Desfrançois, C.; Abdoul-Carime, H.; Schermann, J.-P. *Int. J. Mol. Phys. B* **1996**, *10*, 1339.
(27) Dang, L. X.; Chang, T.-M. *J. Chem. Phys.* **1996**, *106*, 8149.
(28) Schnitker, R.; Rossky, P. J. *J. Chem. Phys.* **1986**, *86*, 3462.

(29) Koopmans, T. *Physica* **1933**, *1*, 104.
(30) Sommerfeld, T. *J. Chem. Phys.* **2004**, *121*, 4097.
(31) Saad, Y. *Numerical Methods for Large Eigenvalue Problems*; Manchester University Press: Manchester, U.K., 1992.
(32) Neirotti, J. P.; Calvo, F.; Freeman, D. L.; Doll, J. D. *J. Chem. Phys.* **2000**, *112*, 10340.
(33) Tsai, C. J.; Jordan, K. D. *J. Phys. Chem.* **1993**, *97*, 5208.
(34) Hartke, B. *Phys. Chem. Chem. Phys.* **2003**, *5*, 275.
(35) The 20 temperatures in the parallel-tempering Monte Carlo calculations are 25, 26, 28, 31, 35, 40, 46, 53, 61, 70, 80, 92, 106, 122, 140, 160, 182, 205, 230, and 260 K.
(36) Metropolis, N.; Rosenbluth, A. W.; Rosenbluth, M. N.; Teller, A. H.; Teller, E. *J. Chem. Phys.* **1953**, *21*, 1087.
(37) Turi, L.; Sheu, W. S.; Rossky, P. J. *Science* **2005**, *309*, 914.